



# Heavy metal concentrations differ along wetland-to-grassland soils: a case study in an ecological transition zone in Hulunbuir, Inner Mongolia

Junyong Ma<sup>1,2,3</sup> · Zhenzhen Hao<sup>1,2</sup> · Yibo Sun<sup>1,2</sup> · Bo Liu<sup>1,2</sup> · Wenjie Jing<sup>1,2</sup> · Jiaqiang Du<sup>1,2</sup> · Junsheng Li<sup>1,2</sup>

Received: 9 August 2021 / Accepted: 27 December 2021 / Published online: 22 January 2022  
© The Author(s), under exclusive licence to Springer-Verlag GmbH Germany, part of Springer Nature 2022

## Abstract

**Purpose** Ecosystem changes occurring against a backdrop of climate changes have set off a chain reaction through the cycle of matter and energy affecting water, soils, and plants. Heavy metal elements have long been research hotspots due to their unique impacts on the composition and function of soils and plants. Most studies of heavy metals are conducted in contaminated industrial and residential areas, but more studies need to be conducted on well-protected nature reserves undergoing ecological transition.

**Method** This study was conducted in a wetland-to-grassland ecotone in the Huihe National Nature Reserve, Inner Mongolia, where wetland has been decreasing and turning into grassland in the past few decades. To compare associations between the grasslandification of wetland and the presence of heavy metals, concentration of 11 heavy metals [iron (Fe), copper (Cu), zinc (Zn), manganese (Mn), nickel (Ni), vanadium (V), antimony (Sb), arsenic (As), chromium (Cr), cadmium (Cd), and lead (Pb)], vegetation characteristics (above and belowground plant biomass, height, and species), and topsoil (0–20 cm) characteristics [pH, electrical conductivity (EC), soil moisture, bulk density, and concentration of P, K, Ca, Na, and Mg] were measured at four independent sites, each of which contained three kinds of ecosystems (i.e., treatments): wetlands, wetland-grassland junctions, and grasslands.

**Results** Soil Fe, Cr, and Pb concentrations increased as the ecotype shifted from wetland to grassland, whereas Mn and Cd decreased. SW (soil water) and pH levels also decreased; the SW value was the highest in the wetlands ( $32.8 \pm 3.63\%$ ) and decreased from the junction lands ( $30.6 \pm 4.7\%$ ) to the grasslands ( $22.1 \pm 2.85\%$ ) ( $p < 0.01$ ); and pH decreased from 8.9 to 7.8 from the wetlands to the adjacent wetlands ( $p < 0.01$ ). Plant coverage and aboveground biomass levels were highest in the wetland plots, whereas belowground biomass levels were highest in the grassland plots.

**Conclusions** Even though little human disturbance occurs in the grassland-to-wetland ecosystems in the nature reserves of Huihe Hulunbuir, Inner Mongolia, trace amounts of heavy metals were still detected (Fe, Cr, Pb, Mn, and Cd). Shifts in soil water and pH may be responsible for this phenomenon.

**Keywords** Ecosystem change · Soil heavy metals · Soil moisture · Soil pH

## 1 Introduction

Global warming and land usage have caused considerable ecosystem changes in recent years (Meyfroidt and Lambin 2011; Horion et al. 2019), including wetland loss

and grassland degradation (Niu et al. 2012; Dong et al. 2012; Nguyen et al. 2016; Yang et al. 2016). The natural wetland area of China decreased by approximately 33% between 1978 and 2008 based on remote sensing data and, of this, riverine and lacustrine wetlands constituted the majority of wetland loss (Niu et al. 2012). Environmental processes cause changes in ecosystems, producing a series of chain reactions that affect biodiversity (García-Palacios et al. 2018), ecosystem services (Charles and Dukes 2008), and net primary productivity (Costanza et al. 2007).

Responsible editor: Claudio Colombo

✉ Junsheng Li  
lijsh@craes.org.cn

Extended author information available on the last page of the article

Soil material is one of the foundations of an ecosystem (Rillig and Mummey 2010; Adhikari and Hartemink 2016; Faucon et al. 2017). Moreover, research on natural ecosystems and soil often focuses on soil carbon and nitrogen cycling (Batlle-Aguilar et al. 2011), soil microorganisms (Lorenzo et al. 2010), and the soil rhizosphere (Cardon and Whitbeck 2011). Heavy metals levels in soil have mostly been studied in areas of high population density or in places with a high likelihood of anthropogenic pollution such as mining areas (Li et al. 2014), industrial areas (Yaylali-Abanuz 2011), agricultural irrigation zones (Zhang et al. 2018), and transportation/railway areas (Zhang et al. 2018). However, relatively few have focused on natural reserve areas where toxic metals can accumulate and then never degrade. Heavy metals settle in soils and vegetation through dry and wet deposition (Zhang et al. 2018). Studies have been done on ecosystem services (Zhang et al. 2019a, b), biodiversity (Xu et al. 2017), and carbon and nitrogen cycles (Gao et al. 2020) in nature reserves, which accounted for 18% of the geographic area of China until the year 2020 (Sun et al. 2020). Yet, this research did not focus on heavy metal levels in the soil. In nature reserves, heavy metal pollution is generally restricted by local regulations, but natural processes can still contribute heavy metals to the soil.

Essential heavy metals are necessary for the proper function of biological systems (Dai et al. 2004; Chen et al. 2010; Seth 2012; Sarwar et al. 2017). Low concentrations of elements like copper (Cu), zinc (Zn), manganese (Mn), nickel (Ni), and iron (Fe) are required by plants for proper growth (Fageria et al. 2009) and have important regulatory roles in a number of biological processes such as electron transfer and enzymatic reactions (Fageria et al. 2009; Chaffai and Koyama 2011). Non-essential metals with no known biological functions in plants are antimony (Sb), arsenic (As), chromium (Cr), silver (Ag), cadmium (Cd), mercury (Hg), and lead (Pb) (Viehweger 2014). Excessive levels of these non-essential metals are toxic to plants and can inhibit growth, deteriorate soil quality, reduce yield, and lead to the production of poor quality or toxic crops (Seth et al. 2007; Choppala et al. 2014).

As a part of the Eurasian steppe landscape, the Hulunbuir grassland encompasses multiple ecosystem types such as grassland, wetland, forest, and sandy land. It is naturally an ecologically sensitive and vulnerable region, but global climate change has exacerbated these problems (Bai et al. 2008; Hu et al. 2015). This area provides crucial ecosystem services including windbreak provision, sand fixation, and water conservation in northern China. It is also rich in biodiversity and an important habitat for migratory birds.

The Huihe National Nature Reserve is a mosaic of wetlands and grasslands found adjacent to each other. The distribution of these wetlands and grasslands depends on

topography, precipitation, and temperature (He et al. 2018). Climate change, especially the frequent occurrence of drought, had caused the loss of wetlands, the reduction of plant species diversity, and land desertification in the Hulunbuir grassland region (Li et al. 2018; Na et al. 2019; Zhou et al. 2019). To understand how heavy metals are distributed throughout wetlands and grasslands undergoing an ecological transition the correlation between ecosystem type and heavy metal concentrations in the wetland-to-grassland soils of the Huihe National Nature Reserve in Hulunbuir, Inner Mongolia, during August 2020 through a regional scale plot-based field investigation and laboratory chemical analyses. Forty-eight plots in four separate sites were selected and studied. At each site, topsoil (0–20 cm) was sampled and vegetation structure data was collected from three wetland plots and three grassland plots (3 m\*3 m).

The hypotheses of this work are as follows: (1) some soil heavy metal concentrations differ between wetlands and grasslands, even in the well protected ecological transition zone of Hulunbuir, Inner Mongolia; (2) changes in soil water affect pH and plant biomass levels in wetland-to-grassland transition zones; and (3) environmental factors have the greatest effect on soil heavy metal concentrations.

## 2 Materials and methods

### 2.1 Study area

The research area is located in Hulunbuir Huihe National Nature Reserve of Inner Mongolia, China (48°10'50" ~ 48°57'00" N, 118°47'30" ~ 119°41'27" E, 600–750 m above sea level). The study area has a temperate continental monsoon climate with annual average temperatures ranging from –2.4 to 2.2 °C. The study site has long and cold winters and relatively warm and short summers with a frost-free period ranging from 100 to 120 days. Annual precipitation levels reach is 300–350 mm. Of this, over 70% fall between June and August (Fig. 1). Fluvisols and Kastanozems are the main types of soils in the research area (IUSS Working Group WRB 2014).

### 2.2 Sampling design

Soil samples and data on vegetation characteristics were collected during August 2020. To evaluate ecological factors and heavy metal concentrations in the soil, four sampling sites were selected near one of three wetland types: (1) HH and TM sites which are close to rivers; (2) HG and XP sites, both of which are contained within lakes (Table 1).

Sample plots were set up in wetland areas, grassland areas, and wetland-grassland areas which were at the junction between these two habitats (Supplementary Fig. 1).

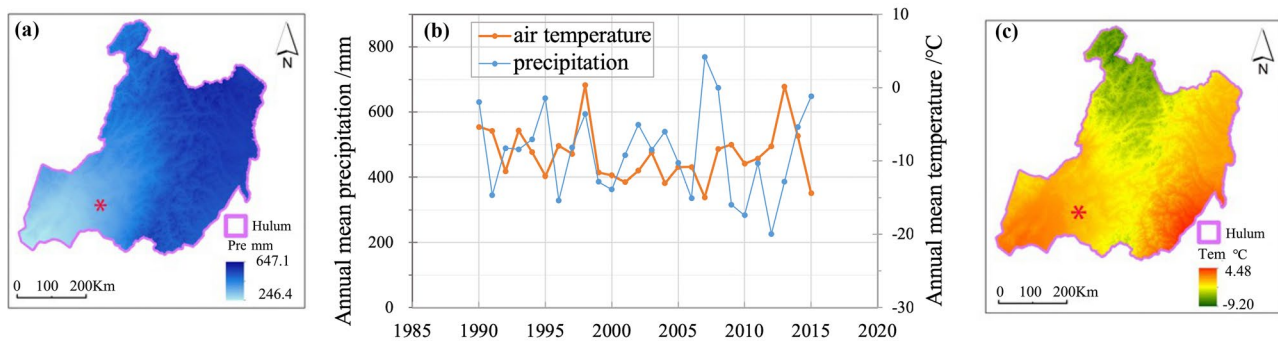


**Fig. 1** Annual mean precipitation and temperature in Hulunbuir, Inner Mongolia. **(a)** Annual mean precipitation in the Hulunbuir area (1990–2015); **(b)** Trends in precipitation and air temperature (1990–

2015); **(c)** Annual mean temperature in Hulunbuir area (1990–2015). The red marker “\*” represents the study area location in the Huihe National Nature Reserve

Four 3 m\*3 m replicate plots spaced 50 m apart were set up in each of the three areas. Thus, every sampling site contained three kinds of plots: (1) wetland plots; (2) wetland-grassland junction plots; and (3) grassland plots. An RTK (GPS, South Mapping Galaxy I. China) was used to get the accurate positioning data including geodetic coordinates (LAT, LON) for all 48 plots across the four different sites. The definitions and the estimates of topographic properties are presented in Table 1. More detailed information is presented in Supplementary Table 1.

### 2.3 Data collection

Three random replicates of surface soil were collected from each sampling plot using a rectangular soil sampler (10 cm long × 10 cm wide × 20 cm deep). Humus layer samples were sieved through a 2-mm mesh sieve. This step removed live roots, mycorrhizal mycelia, and coarse plant remnants. The treated soil sample was then divided into two parts, one of which was kept fresh and the other of which was kept dry. In each sample plot, two soil samples were collected from the middle of the surface soil profile (0–20 cm) using a ring cutter (100 m<sup>-3</sup>).

Aboveground biomass (AGB) was measured by harvesting all aboveground plant material in a 0.25 m × 0.25 m subplot, and belowground biomass (BGB) was collected using an excavation method. All the AGB parts of the green plant were dried for 30 min at 105 °C within 1 day after excavation before being transferred to the laboratory. BGB was sampled by extracting a soil cylinder approximately 25 cm in diameter and collecting plant matter based on local root depth (0~40 cm of soil). BGB matter was carefully collected and separated from the soil and other belowground material. No distinguishment was made between living and dead roots. The samples were passed through a 0.5-mm mesh sieve and then washed with purified water. Both AGB and BGB

samples were dried in an oven (75 °C) until a constant biomass was achieved to calculate dry biomass.

### 2.4 Laboratory analysis

Soil was air-dried and passed through a 2-mm mesh sieve prior to analysis. Three grams of soil were mixed with distilled water (1:2.5, w/v) for 30 min and a pH meter was used to determine pH. Soil water (SW) concentrations were calculated as the loss of mass from fresh soil (10 ± 0.5 g) over 24 h of drying at 105 °C in aluminum cans until the weight was constant.

The soil was air-dried and passed through a 0.15-mm mesh sieve prior to metal concentration analysis (P, K, Ca, Mg, Na, V, Cr, Fe, Mn, Co, Ni, Cu, Zn, As, Mo, Cd, and Sb were measured) based on the national standard method of China (HJ 803–2016). Soil samples were digested in a mixture of concentrated HCl, HNO<sub>3</sub>, H<sub>2</sub>O<sub>2</sub>, and HF at 180 °C using a microwave oven (Ethos Touch Control, Milestone Inc., Italy). The digested solutions were diluted with deionized water prior to chemical analysis. Inductively coupled plasma mass spectrometry (ICP-MS 7800 and ICP-OES 5800, Agilent, USA) was used to measure the levels of metal in prepared samples and in natural standard reference soil after every 10 measurements (GBW 07406). The national research center for certified reference materials in China was consulted to assure the quality of testing.

### 2.5 Data analysis

R (version 4.0.0) (R Core Team 2020) was used for statistical analyses and data visualization. Each of the 48 plots was considered an experimental unit, and the four replicate plots were averaged before performing statistical analyses. Prior to conducting ANOVA, the assumption of normality (Kolmogorov–Smirnov test) and homogeneity (Levene’s test) was checked for each variable. For each site, ANOVA was

**Table 1** Basic information for the study plots

Plots and treatments	Geographical location			Plant Dominant species	Soil				
	Latitude (N)	Longitude (E)	Altitude m		Ca (mg kg <sup>-1</sup> )	K (mg kg <sup>-1</sup> )	Na (mg kg <sup>-1</sup> )	P (mg kg <sup>-1</sup> )	Mg (mg kg <sup>-1</sup> )
HH-Wetland-1	48°13'11.86"N	119°15'37.52"E	717	<i>Leymus chinensis</i> Tzvel	71,236	10,000	6950	14,602	1587
HH-Wetland-2	48°13'13.08"N	119°15'40.67"E	716	<i>Leymus chinensis</i> Tzvel	62,872	11,155	6893	6036	1680
HH-Wetland-3	48°13'14.02"N	119°15'43.92"E	716	<i>Leymus chinensis</i> Tzvel	37,488	15,030	8360	12,431	1714
HH-Wetland-4	48°13'15.18"N	119°15'47.25"E	715	<i>Leymus chinensis</i> Tzvel	57,198	12,061	7401	11,023	1660
HH-Junction-1	48°13'10.68"N	119°15'39.17"E	718	<i>Leymus chinensis</i> Tzvel	36,131	17,377	9965	7001	1062
HH-Junction-2	48°13'11.51"N	119°15'41.61"E	720	<i>Leymus chinensis</i> Tzvel	32,150	17,147	10,314	4589	1120
HH-Junction-3	48°13'12.23"N	119°15'44.46"E	717	<i>Leymus chinensis</i> Tzvel	19,383	19,356	10,665	6299	1101
HH-Junction-4	48°13'13.13"N	119°15'47.19"E	718	<i>Leymus chinensis</i> Tzvel	29,220	17,960	10,314	5963	1093
HH-Grassland-1	48°13'9.86"N	119°15'40.22"E	722	<i>Leymus chinensis</i> Tzvel	970	24,651	12,817	1401	518
HH-Grassland-2	48°13'10.69"N	119°15'42.55"E	722	<i>Leymus chinensis</i> Tzvel	1264	22,951	13,537	1123	542
HH-Grassland-3	48°13'10.39"N	119°15'40.65"E	721	<i>Leymus chinensis</i> Tzvel	1153	23,606	12,902	2158	481
HH-Grassland-4	48°13'11.71"N	119°15'47.46"E	722	<i>Leymus chinensis</i> Tzvel	1128	23,735	13,085	1560	514
HG-Wetland-1	48°26'16.65"N	119° 9'1.17"E	681	<i>Leymus chinensis</i> Tzvel	37,369	15,123	11,092	9305	951
HG-Wetland-2	48°26'15.02"N	119° 9'1.06"E	681	<i>Leymus chinensis</i> Tzvel	33,578	18,727	11,159	4829	970
HG-Wetland-3	48°26'13.46"N	119° 9'0.90"E	680	<i>Leymus chinensis</i> Tzvel	20,105	20,610	11,701	8411	1001
HG-Wetland-4	48°26'12.27"N	119° 9'0.66"E	680	<i>Leymus chinensis</i> Tzvel	30,349	18,153	11,317	7515	973
HG-Junction-1	48°26'16.47"N	119° 9'4.87"E	680	<i>Leymus chinensis</i> Tzvel	19,290	18,736	13,706	4169	656
HG-Junction-2	48°26'14.64"N	119° 9'4.71"E	681	<i>Leymus chinensis</i> Tzvel	17,418	21,590	13,663	3864	668
HG-Junction-3	48°26'13.23"N	119° 9'4.53"E	682	<i>Leymus chinensis</i> Tzvel	10,605	21,289	13,782	4935	675
HG-Junction-4	48°26'12.02"N	119° 9'3.91"E	681	<i>Leymus chinensis</i> Tzvel	15,771	20,538	13,717	4322	666
HG-Grassland-1	48°26'16.13"N	119° 9'8.17"E	682	<i>Leymus chinensis</i> Tzvel	1076	22,326	16,251	1027	354
HG-Grassland-2	48°26'14.30"N	119° 9'7.76"E	682	<i>Leymus chinensis</i> Tzvel	1173	24,318	16,076	894	345
HG-Grassland-3	48°26'12.91"N	119° 9'7.32"E	683	<i>Leymus chinensis</i> Tzvel	993	21,804	15,773	1440	330
HG-Grassland-4	48°26'11.71"N	119° 9'6.87"E	682	<i>Leymus chinensis</i> Tzvel	1079	22,816	16,032	1120	342
XP-Wetland-1	48°48'52.12"N	119°22'22.74"E	644	<i>Leymus chinensis</i> Tzvel	6501	20,244	15,232	4005	313
XP-Wetland-2	48°48'53.02"N	119°22'38.36"E	643	<i>Leymus chinensis</i> Tzvel	4282	26,300	15,423	3622	259

**Table 1** (continued)

Plots and treatments	Geographical location			Plant Dominant species	Soil				
	Latitude (N)	Longitude (E)	Altitude m		Ca (mg kg <sup>-1</sup> )	K (mg kg <sup>-1</sup> )	Na (mg kg <sup>-1</sup> )	P (mg kg <sup>-1</sup> )	Mg (mg kg <sup>-1</sup> )
XP-Wetland-3	48°48'54.85"N	119°22'56.49"E	644	<i>Leymus chinensis</i> Tzvel	4721	26,189	15,042	4389	288
XP-Wetland-4	48°48'59.84"N	119°23'30.33"E	644	<i>Leymus chinensis</i> Tzvel	5167	24,244	15,232	4005	286
XP-Junction-1	48°48'48.56"N	119°22'23.46"E	647	<i>Leymus chinensis</i> Tzvel	3852	23,368	17,530	2335	270
XP-Junction-2	48°48'48.86"N	119°22'38.62"E	644	<i>Leymus chinensis</i> Tzvel	2701	26,068	17,022	2149	210
XP-Junction-3	48°48'50.79"N	119°22'56.66"E	645	<i>Potentilla acaulis</i> L	2807	27,060	16,932	2560	243
XP-Junction-4	48°48'54.68"N	119°23'30.19"E	645	<i>Potentilla acaulis</i> L	3119	25,498	17,161	2348	241
XP-Grassland-1	48°48'45.02"N	119°22'23.79"E	649	<i>Potentilla acaulis</i> L	1181	26,387	19,684	652	188
XP-Grassland-2	48°48'45.47"N	119°22'38.84"E	647	<i>Potentilla acaulis</i> L	1081	25,685	18,614	665	148
XP-Grassland-3	48°48'46.97"N	119°22'56.34"E	646	<i>Leymus chinensis</i> Tzvel	831	27,791	18,642	721	178
XP-Grassland-4	48°48'49.02"N	119°23'30.04"E	647	<i>Leymus chinensis</i> Tzvel	1031	26,620	18,980	679	171
TM-Wetland-1	48°55'45.43"N	119°40'29.46"E	636	<i>Iris ensata</i> Thunb	24,559	21,691	18,572	18,923	607
TM-Wetland-2	48°55'19.87"N	119°39'56.25"E	633	<i>Leymus chinensis</i> Tzvel	26,003	20,259	12,579	13,101	984
TM-Wetland-3	48°55'17.98"N	119°39'28.37"E	637	<i>Leymus chinensis</i> Tzvel	17,446	23,826	14,585	17,279	560
TM-Wetland-4	48°55'39.31"N	119°40'23.99"E	634	<i>Leymus chinensis</i> Tzvel	22,669	21,925	15,245	16,433	717
TM-Junction-1	48°55'45.42"N	119°40'23.71"E	634	<i>Leymus chinensis</i> Tzvel	21,838	22,500	16,377	13,227	545
TM-Junction-2	48°55'23.00"N	119°39'52.76"E	632	<i>Suaeda glauca</i> Bunge	19,522	22,249	15,721	11,541	835
TM-Junction-3	48°55'21.17"N	119°39'26.97"E	643	<i>Leymus chinensis</i> Tzvel	16,097	24,668	14,784	13,228	611
TM-Junction-4	48°55'39.31"N	119°40'17.88"E	636	<i>Suaeda glauca</i> Bunge	19,152	23,139	15,627	12,665	663
TM-Grassland-1	48°55'45.67"N	119°40'18.95"E	635	<i>Suaeda glauca</i> Bunge	18,955	23,284	14,107	7413	428
TM-Grassland-2	48°55'25.57"N	119°39'50.35"E	634	<i>Leymus chinensis</i> Tzvel	12,948	24,144	18,674	9818	630
TM-Grassland-3	48°55'24.91"N	119°39'25.51"E	653	<i>Leymus chinensis</i> Tzvel	14,560	25,415	14,839	8987	625
TM-Grassland-4	48°55'39.11"N	119°40'11.89"E	640	<i>Leymus chinensis</i> Tzvel	15,487	24,281	15,873	8739	560

Four sites were selected (HH, HG, XP, and TM). In each site, 3 wetland plots and 3 grassland plots were established and sampled. All data were collected in August 2020

used to compare the environmental variables of grassland and wetland ecosystems. Two-way ANOVA was performed to compare environmental variables among both the treatments (two ecosystems: wetland and the grassland) and sampling

sites (four locations). All results are represented as mean value  $\pm$  standard error. Pearson correlations were analyzed using R, and the data was visualized using the “Performance Analytics” package.

**Table 2** Tests of differences among the plots based on one-way ANOVA

	df	Fe	K	P	V	Cr	Mn	Co	Ni	Cu	Zn	As
Plots	3	<0.001	<0.001	<0.001	<0.001	<0.001	<0.001	<0.001	<0.001	<0.001	<0.001	<0.001
Treatments	2	<0.001	<0.001	<0.001	<0.001	<0.001	<0.001	0.038	0.559	0.320	0.001	0.515
Plot*Treat	6	0.273	<0.001	<0.001	0.010	0.939	<0.001	0.084	0.225	0.030	0.936	0.230
	df	Mo	Cd	Sb	Pb	pH	SW	Cover	Height	TB	AGB	BGB
Plots	3	<0.001	<0.001	<0.001	0.007	<0.001	<0.001	<0.001	<0.001	<0.001	<0.001	<0.001
Treatment	2	0.173	<0.001	0.031	0.001	<0.001	<0.001	<0.001	<0.001	<0.001	<0.001	<0.001
Plot*Treat	6	0.194	0.007	0.318	0.001	0.150	0.259	0.042	<0.001	0.630	<0.001	0.132

Plots mean the *p* value group the data from the same site (e.g., HH, TM; *n*=6) and conducted one-way ANOVA. SW, soil water; Height, plant average height; TB, plant total biomass; AGB, aboveground biomass; BGB, belowground biomass. Treatments mean the *p* value group the data from the same treatment (grassland, junction, and wetland; *n*=12) and conducted one-way ANOVA

### 3 Results

#### 3.1 Soil trace heavy metals

##### 3.1.1 Soil Fe, Cr, and Pb concentrations decreased as wetland transitioned into grassland

Fe and Mn decreased significantly between grassland, grassland-wetland junction, and wetland soils at the study sites (Table 2). The concentration of Fe is 22.2% greater in wetland than in adjacent grassland soils ( $11,374 \pm 1621.39 \text{ mg kg}^{-1}$ ,  $12,552.6 \pm 866.19 \text{ mg kg}^{-1}$ , and  $13,903.2 \pm 1260.92 \text{ mg kg}^{-1}$  in wetland, junction, and grassland soils, respectively) (Fig. 2a). By contrast,

the concentration of Cr is  $19.8 \pm 3.3 \text{ mg kg}^{-1}$  in wetland soil and  $28.9 \pm 2.7 \text{ mg kg}^{-1}$  in grassland soil. Cr concentration was also significantly different between all three sites ( $p < 0.001$ ) (Fig. 2b). In two out of the four sites in which Pb decreased significantly, the concentration of Pb was 13.3% lower in wetland than in grassland soil ( $16.2 \pm 0.82 \text{ mg kg}^{-1}$  soil) (Fig. 2c).

##### 3.1.2 Soil Mn and Cd concentrations increased as wetland transitioned into grassland

On average, the concentration of Mn was 28.7% higher in wetland than in grassland soils ( $452.3 \pm 163.73 \text{ mg kg}^{-1}$ ,  $383.6 \pm 25.38 \text{ mg kg}^{-1}$ ,  $322.6 \pm 30.97 \text{ mg kg}^{-1}$  for wetland,

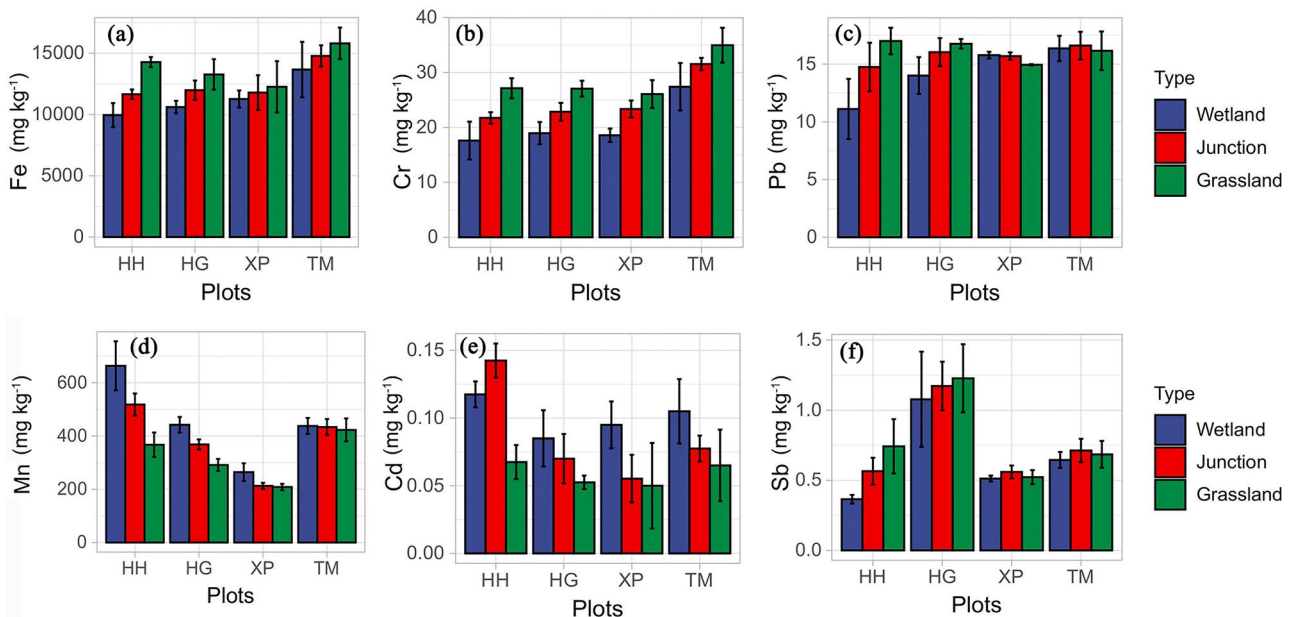


**Fig. 2** Heavy metal concentrations in wetland and grassland soils of at the four study sites. (a) soil total Ferrum metal concentration; (b) Chromium metal; (c) Plumbum metal; (d) Manganese metal; (e) Cad-

mium metal; (f) Stibonium metal. HH, HG, XP, and TM represent the four selected sites (*n*=4 plots were used for each site-ecosystem combination). All data were collected in August 2020



junction, and grassland soils, respectively). Mn significantly increased from wetlands to grasslands at the HG and XP sites and generally increased at all four sites (Fig. 2d; Table 2). Cd was similar to Mn, in that it increased by 28.7% from wetlands to grasslands ( $0.10 \pm 0.014 \text{ mg kg}^{-1}$ ,  $0.09 \pm 0.015 \text{ mg kg}^{-1}$ ,  $0.06 \pm 0.019 \text{ mg kg}^{-1}$  for wetland, junction, and grassland soils) (Fig. 2e). Levels of other trace heavy metal elements changed, as well, but the differences were not significant (Supplementary Fig. 2).

### 3.2 Soil as an environmental variable

Each of the three ecosystems had different environmental factors. pH increased significantly from wetland to junctionland to grassland. SW was lower (wetland:  $32.8 \pm 3.63$ ; junction land:  $30.6 \pm 4.7\%$ ; grassland:  $22.1 \pm 2.85\%$ ,  $p < 0.01$ ,  $n = 16$ ) and pH higher (from  $8.9 \pm 0.7$  to  $7.8 \pm 0.9$ ) in the grassland plots than in adjacent wetlands at all four study sites (Fig. 3a, b). P concentrations were 50.7% greater in the wetlands than the grasslands ( $p < 0.001$ ), and K concentrations were 34.0% higher in the wetlands. Both P and K were affected by the study site, the ecosystem treatment, and the interaction between study site and ecosystem treatment effects (Fig. 3c, d).

### 3.3 Plant as an environmental variable

Vegetative coverage and the ABG index varied significantly among the sites and increased from the wetlands to the adjacent grasslands. Vegetative cover was  $79 \pm 13.0\%$  vs  $75 \pm 5.7\%$ ,  $64 \pm 2.4\%$  on average in wetland, junction land, and grassland, respectively (Fig. 3e). Plant average height

showed with a pattern like that of the vegetative coverage. ABG was 40.9% higher in the four wetland sites on average ( $96 \pm 47.7 \text{ g m}^{-2}$ ) than it was in the four grassland sites ( $57 \pm 8.8 \text{ g m}^{-2}$ ;  $p < 0.001$ ) (Fig. 3g). However, BGB in the wetland sites ( $351 \pm 47.9 \text{ g m}^{-2}$ ) was significantly ( $p < 0.001$ ) lower than it was in the grassland sites ( $667 \pm 68.5 \text{ g m}^{-2}$ ) (Fig. 3h).

### 3.4 Correlations between variables

The concentration of Fe was significantly, positively, and strongly correlated with Cr ( $R = 0.83$ ,  $n = 48$ ,  $p < 0.01$ ), Co ( $R = 0.670$ ,  $n = 48$ ,  $p < 0.01$ ), Pb ( $R = 0.63$ ,  $n = 48$ ,  $p < 0.01$ ), and total plant biomass ( $R = 0.65$ ,  $n = 48$ ,  $p < 0.01$ ) but was negatively correlated with plant coverage ( $R = -0.78$ ,  $n = 48$ ,  $p < 0.01$ ). Mn was correlated with Ca ( $R = 0.87$ ,  $n = 48$ ,  $p < 0.01$ ), P ( $R = 0.902$ ,  $n = 24$ ,  $p < 0.01$ ), SW ( $R = 0.65$ ,  $n = 48$ ,  $p < 0.01$ ), Zn ( $R = 0.712$ ,  $n = 24$ ,  $p < 0.01$ ), and Cd ( $R = 0.649$ ,  $n = 24$ ,  $p < 0.01$ ) but was negatively correlated with K ( $R = -0.907$ ,  $n = 24$ ,  $p < 0.01$ ), Na ( $R = -0.841$ ,  $n = 24$ ,  $p < 0.01$ ), and Pb ( $R = -0.579$ ,  $n = 24$ ,  $p < 0.01$ ) (Fig. 4).

## 4 Discussion

Generally, heavy metal concentrations in soils of the Huihe Nature Reserve did not exceed benchmarks set by the local environmental protection agency (GB 15618–2018). Heavy metal elements are less involved in the plant-soil cycle than organic elements (C, N, P, K) (Manlay et al. 2002;

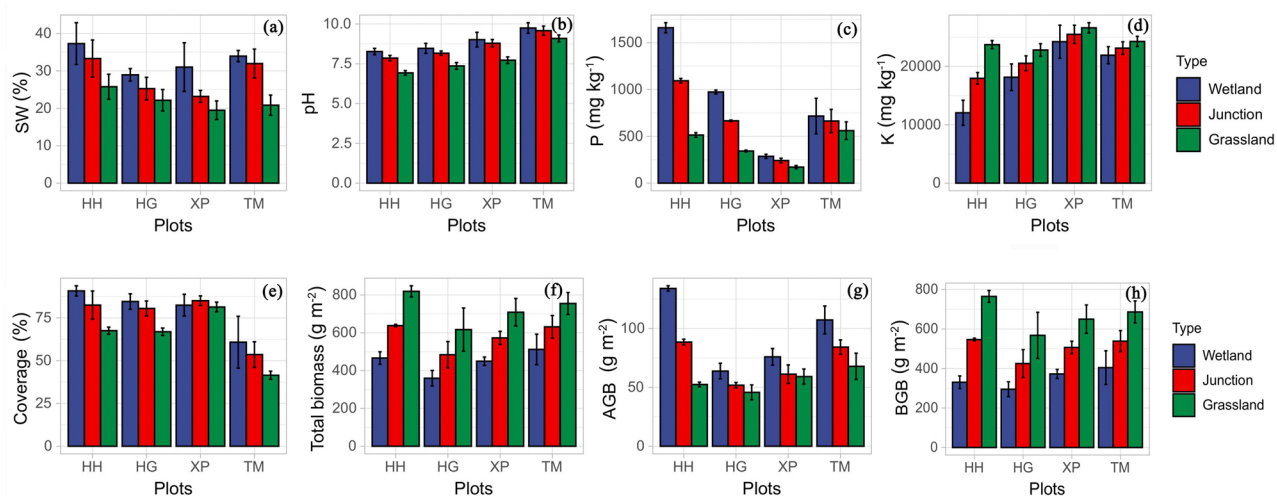
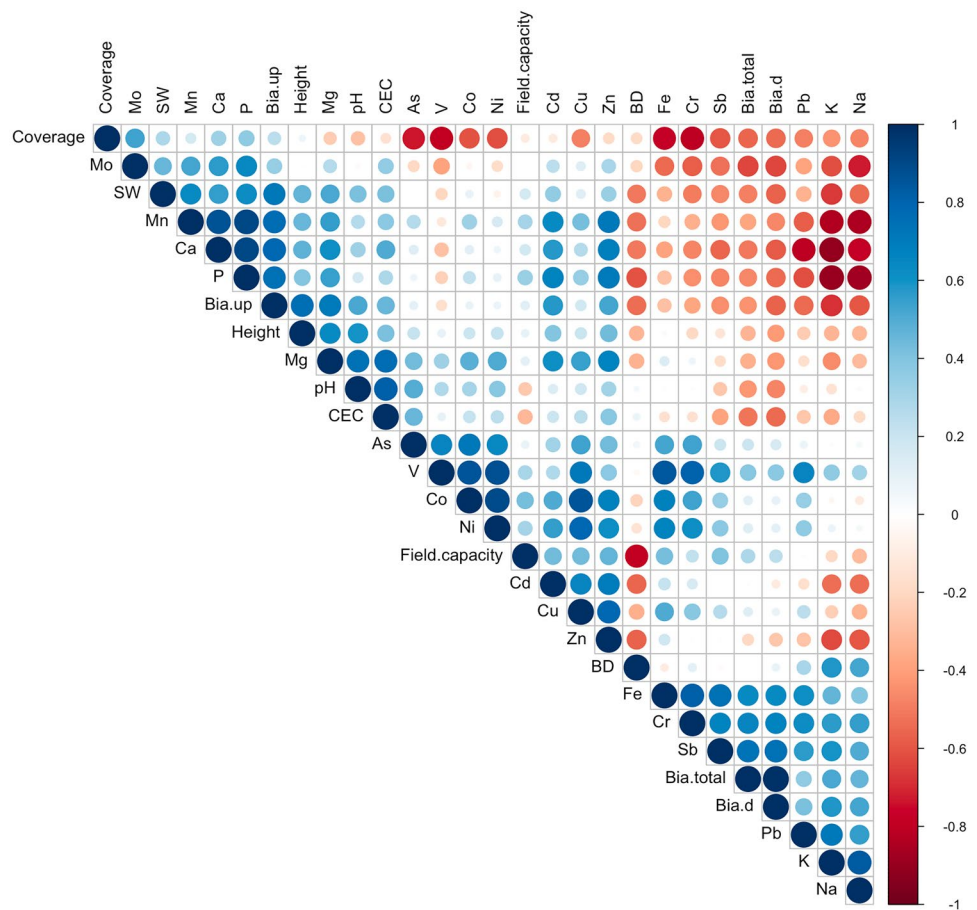


**Fig. 3** Environmental variables in wetland, wetland-to-grassland junction, to grassland plots at the four study sites. **(a)** soil water content; **(b)** soil pH; **(c)** soil total phosphorus concentration; **(d)** soil total potassium concentration; **(e)** plant average coverage; **(f)** total

plant biomass; **(g)** above-ground biomass; **(h)** below-ground biomass. Error bars represent the standard error of the replicate plots. HH, HG, XP, and TM represent the four selected sites (at each site,  $n = 4$ ). All data were collected in August 2020

**Fig. 4** Pearson correlation coefficient thermal maps of physical, chemical, and biological indexes across wetland, plots junction, and grassland plots. The deep red color represents the strongest strong positive correlation (coefficient  $R = 1$ ), the deep blue color represents the strongest strong negatively correlation ( $R = -1$ ), and the pure white means that there was no correlation ( $R = 0$ ) between the two indicators. For each index,  $n = 48$



Kallenbach et al. 2019). However, soil composition, plant density, and the concentrations of some heavy metals were significantly affected by environment type (i.e., wetland, wet-grassland junction, and grassland).

#### 4.1 Environmental factors affecting water and soil pH dynamics

From 1960 to 2017, the average annual precipitation level of the Hulunbuir grassland decreased by 3.65 mm every 10 years (Zhang et al. 2019a, b). In addition to decreasing precipitation levels, topology changed across the landscape. At all four sites, the grasslands were at a slightly higher elevation than both the adjacent wetland-grassland junctions and the wetlands. Precipitation levels and topology could have affected SW which changed significantly from wetlands to junction lands to grasslands. SW affects plant vegetative cover, plant height, and AGB levels (Liu et al. 2010; Deng et al. 2016), as well as plant diversity levels which were positively correlated with SW in this study (Fig. 4). Thus, changes in SW may cause wetlands to change into grasslands over time.

Generally, the Hulunbuir study site has a strong water conservation capacity as it is covered by over 3,000 rivers

and 500 lakes (Yu et al. 2015). Strong evaporation and transpiration rates (Sun et al. 2016) cause the aeration zones of shallow groundwater to accumulate salt at a rapid rate. Thus, the soil salt content in this region is high. Evaporation leads to a continuous increase in the concentration of alkali metals and salt in groundwater (Risacher et al. 2003). This could have caused the pH of the wetland ecosystem to reach 8.9 and the SW to reach 32.9%, compared with grassland where the pH is 7.8 and the SW is 22.1% based on this study.

These plot-level studies could partly explain why the pH-EC dynamics changed between wetlands, wetland-grassland junctions, and grasslands. In this study, soil Ca and Mg concentrations were over 10 and 5 times higher, respectively, in the wetlands than they were in the nearby grasslands. The pH and EC levels also decreased from the wetlands to the junction plots to the grassland plots. This could have happened because Ca and Mg directly influence soil base saturation, pH, and EC levels. Since soil pH was positively and significantly correlated with exchangeable  $K^+$ ,  $Ca^{2+}$ , and  $Mg^{2+}$  levels, this study further reinforces that these environmental factors interact with one another (Behera and Shukla 2015).

The pH values were positively correlated with EC ( $R = 0.81, p < 0.001$ ) (Fig. 4), in that stronger soil conductance



more likely to be found in alkaline soils. Soil salinization restricts the sustainable use of land and the stability of the ecosystem (Scudiero et al. 2016), especially in arid and semi-arid regions with low precipitation and high evaporation rates (Wichelns and Qadir 2015). Recent studies suggest that the pH may alter the environment of microorganisms, affecting the material and structural characteristics of the soil. Sediment samples taken from 15 lakes on the Tibetan Plateau showed that pH is the best predictor of bacterial community structure in alkaline sediments (Xiong et al. 2012). Moreover, studies done in the well-conserved, natural ecosystems on Changbai Mountain emphasized that pH predicts how soil bacterial is distributed at different elevations (Shen et al. 2013). pH changes also change the aggregate structure of the soil (Liang et al. 2000; Cornelissen et al. 2018).

#### 4.2 Heavy metal element dynamics in wetland-to-grassland transition zones

Soil Fe availability could be related to redox potential (Colombo et al. 2014). Both high SW content and poor aeration convert ferric iron ( $\text{Fe}^{3+}$ ) to bioavailable iron ( $\text{Fe}^{2+}$ ) (Lindsay 1984). Moreover, Fe deficiency in plants mostly occurs in alkaline soil (Lindsay and Schwab 1982). In this study, Fe levels were positively correlated with BGB and AGB and negatively correlated with increasing soil pH (Fig. 4). The grasslandification of wetlands increased soil Fe concentration and decreased Mn concentration. Changes in these elements were especially apparent because they are found in high abundance in the soil and are easily influenced by environmental factors (Fig. 4 and Supplementary Fig. 2).

Manganese, an important plant nutrient, is involved in photosynthetic pathways (Millaleo et al. 2010). Mn deficiency is more common in sandy soils, in organic soils with a  $\text{pH} > 6$ , and in heavily weathered, tropical soils (Schmidt et al. 2016). Correspondingly, wetland soil had a significantly higher Fe concentration and a higher pH at all four sites. When Mn concentrations within the plant exceed optimal levels, non-essential heavy metals adversely affect the plant as they are unable to be reduced naturally. This causes oxidative stress which ultimately damages cell structures (Asati et al. 2016). The levels of some non-essential metals (Cr, Pb, and Cd) changed slightly from wetlands and grasslands. These metals are toxic, as they can cause severe harm to plants and animals (Rahman and Singh 2019; Seth et al. 2007; Choppala et al. 2014). Cr-induced oxidative stress leads to lipid peroxidation in plants which severely damages the cell membranes (Hayat et al. 2012). Although levels of non-essential metals did not exceed hazardous limits, both Cr and Pb concentrations were greater in grasslands than in adjacent wetlands in three out of the four sites.

In summary, soil Fe, Cr, and Pb concentrations decreased from wetlands to grasslands, whereas soil Mn and Cd

concentrations increased from wetlands to grasslands. Heavy metal elements are often found near mine shafts (Cheng et al. 2019a, b; Tian et al. 2018a, b), railways, and highways (Zhang et al. 2012) where is easy to import more exogenous heavy metal pollutants. For example, road dust from mining areas has a Cd content 60 times greater than normal dust and a Pb content that is nearly 14 times greater. An investigation of long-term agricultural production activities in the Hetao irrigation district indicated that heavy metals accumulated in irrigated soils (Zhu et al. 2017a, b). Excessive levels of these non-essential metals are toxic to plants and can cause growth inhibition, soil quality deterioration, yield reduction, and production of poor quality or toxic agricultural products (Seth et al. 2007; Choppala et al. 2014).

#### 4.3 Belowground plant biomass change

AGB and plant coverage were higher in the wetland plots, whereas BGB was higher in the grassland plots which had neutral, low humidity soil. BGB was negatively correlated with SW in all 48 plots. Since grassland soil contained less SW, roots may have been encouraged to grow deeper to obtain water, resulting in more BGB and more total biomass (TB) in the grassland plots than in the other two ecosystem types.

According to a structural equation model of a semi-arid grassland near the research area, plant coverage and AGB had the strongest, yet also contradictory effects on SW (Yinglan et al. 2019). A gradient analysis conducted in native grasslands across the Loess Plateau, China, on the AGB, BGB, and SW properties of plant communities indicated that higher atmospheric humidity favors greater plant diversity, vegetative cover, AGB, and BGB. In this study, these factors were positively and significantly correlated with soil moisture levels (Deng et al. 2016).

Changes in SW may have had a comprehensive impact on changes in the salinity, alkalinity, and heavy metal content of the soil. This is predicted to have affected plant biomass levels and increased the transition rate of wetland to grassland in a protected nature reserve. Less water might have encouraged grassland root growth and increases underground biomass which led to a higher BGB and TB. In accordance with this observation, the wetland plots had a high-level plant biodiversity and vegetative coverage, whereas the grassland plots had more BGB.

## 5 Conclusion

In the nature reserve of Hulunbuir, Inner Mongolia, the concentrations of some heavy metal elements (Fe, Cr) significantly increased from wetland soil to wetland-grassland junction soil to grassland soil, whereas soil Mn and Cd

concentrations decreased, even though human interference was minimal. Relatively low concentrations of heavy metals among the plots indicate that disturbance from unnatural pollution is controlled well in the reserve. Soil water content, pH, levels of vegetative coverage, and levels of aboveground biomass were higher in the wetlands than in the grasslands, whereas belowground biomass was higher in the grasslands since the plants needed to develop larger root systems to access water. Topography, especially altitude differences, caused the soil water distribution differences, and the loss of precipitation coupled with evapotranspiration due to climate change likely caused the pH differences. The concentrations of some essential soil metals like Fe and Cr and those of non-essential metals like Cd and Mn were changed during the grasslandification of the wetlands.

**Supplementary information** The online version contains supplementary material available at <https://doi.org/10.1007/s11368-021-03132-5>.

**Author contribution** JYM designed experiments, analyzed data and wrote the manuscript. ZZH performed the experiments. JSL provided support for the study area. MJY, WJJ, JQD, JSL, YBS, and BL revised the manuscript.

**Funding** This study was mainly supported by China Postdoctoral Science Foundation (Grant No. 2021M693035). This study was also supported by a Special Fund for Basic Scientific Research Business of Central Public Research Institutes (Grant No. 2019YSKY-017).

## References

- Adhikari K, Hartemink AE (2016) Linking soils to ecosystem services—a global review. *Geoderma* 262:101–111. <https://doi.org/10.1016/j.geoderma.2015.08.009>
- Asati A, Pichhode M, Nikhil K (2016) Effect of heavy metals on plants: an overview. *Int J Appl Innov Eng Manage* 5:2319–4847. <https://doi.org/10.13140/RG.2.2.27583.87204>
- Bai YF, Wu JG, Xing Q et al (2008) Primary production and rain use efficiency across a precipitation gradient on the Mongolia Plateau. *Ecology* 89:2140–2153 <https://doi.org/10.1890/07-0992.1>
- Battle-Aguilar J, Brovelli A, Porporato A et al (2011) Modelling soil carbon and nitrogen cycles during land use change. *Agronomy Sust Developm* 2:499–527. <https://doi.org/10.1051/agro/2010007>
- Behera SK, Shukla AK (2015) Spatial distribution of surface soil acidity, electrical conductivity, soil organic carbon content and exchangeable potassium, calcium and magnesium in some cropped acid soils of India. *Land Degrad Dev* 26(1):71–79
- Cardon ZG, Whitbeck JL (2011) The rhizosphere: an ecological perspective
- Chaffai R, Koyama H (2011) Heavy metal tolerance in *Arabidopsis thaliana*. *Adv Bot Res* 60:1–49. <https://doi.org/10.1016/B978-0-12-385851-1.00001-9>
- Charles H, Duker JS (2008) Impacts of invasive species on ecosystem services. In: Nentwig W. (eds) *Biological invasions. Ecol Stud (analysis and synthesis)* 193:217–237. [https://doi.org/10.1007/978-3-540-36920-2\\_13](https://doi.org/10.1007/978-3-540-36920-2_13)
- Chen G, Zeng G, Du C et al (2010) Transfer of heavy metals from compost to red soil and groundwater under simulated rainfall conditions. *J. Hazard Mater* 181:211–216. <https://doi.org/10.1016/j.jhazmat.2010.04.118>
- Cheng W, Lei SG, Bian ZF et al (2019a) Geographic distribution of heavy metals and identification of their sources in soils near large, open-pit coal mines using positive matrix factorization. *J Hazard Mater* 387:121666. <https://doi.org/10.1016/j.jhazmat.2019.121666>
- Cheng W, Lei SG, Bian ZF, Zhao YB, Li YC, Gan YD (2019b) Geographic distribution of heavy metals and identification of their sources in soils near large, open-pit coal mines using positive matrix factorization. *J Hazard Mater* 121666. <https://doi.org/10.1016/j.jhazmat.2019.121666>
- Choppala G, Saifullah BN et al (2014) Cellular mechanisms in higher plants governing tolerance to cadmium toxicity. *Crit Rev Plant Sci* 33:374–391. <https://doi.org/10.1080/07352689.2014.903747>
- Colombo C, Palumbo G, He JZ (2014) Review on iron availability in soil: interaction of Fe minerals, plants, and microbes. *J Soils Sediments* 14:538–548. <https://doi.org/10.1007/s11368-013-0814-z>
- Cornelissen G, Nurida NL, Hale SE et al (2018) Fading positive effect of biochar on crop yield and soil acidity during five growth seasons in an Indonesian Ultisol. *Sci Total Environ* 634:561–568. <https://doi.org/10.1016/j.scitotenv.2018.03.380>
- Costanza R, Fisher B, Mulder K et al (2007) Biodiversity and ecosystem services: a multi-scale empirical study of the relationship between species richness and net primary production. *Ecol Econ* 61:478–491. <https://doi.org/10.1016/j.ecolecon.2006.03.021>
- Dai J, Becquer T, Rouiller JH et al (2004) Influence of heavy metals on C and N mineralisation and microbial biomass in Zn-, Pb-, Cu-, and Cd-contaminated soils. *Appl Soil Ecol* 25:99–109. <https://doi.org/10.1016/j.apsoil.2003.09.003>
- Deng L, Wang K, Li J et al (2016) Effect of soil moisture and atmospheric humidity on both plant productivity and diversity of native grasslands across the Loess Plateau. *China Ecol Eng* 94:525–531. <https://doi.org/10.1016/j.ecoleng.2016.06.048>
- Dong S-K, Wen L, Li YY et al (2012) Soil-quality effects of grassland degradation and restoration on the Qinghai-Tibetan Plateau. *Soil Sci Soc Am J* 76:2256–2264. <https://doi.org/10.2136/sssaj2012.0092>
- Fageria NK, Barbosa Filho MP, Moreira A et al (2009) Foliar fertilization of crop plants. *J Plant Nutr* 32:1044–1064. <https://doi.org/10.1080/01904160902872826>
- Faucon MP, Houben D, Lambers H (2017) Plant functional traits: soil and ecosystem services. *Trends Plant Sci* 22:385–394. <https://doi.org/10.1016/j.tplants.2017.01.005>
- Gao F, Cui X, Sang Y et al (2020) Changes in soil organic carbon and total nitrogen as affected by primary forest conversion. *For Ecol Manag* 463:118–213. <https://doi.org/10.1016/j.foreco.2020.118013>
- García-Palacios P, Gross N, Gaitán J (2018) Climate mediates the biodiversity–ecosystem stability relationship globally, Proc chromium stress in plants: an overview. *Protoplasma* 249:599–611. <https://doi.org/10.1007/s00709-011-0331-0>
- Hayat S, Khalique G, Irfan M (2012) Physiological changes induced by chromium stress in plants: an overview. *Protoplasma* 249:599–611. <https://doi.org/10.1007/s00709-011-0331-0>
- He J, Su D, Lv S et al (2018) Analysis of factors controlling soil phosphorus loss with surface runoff in Huihe National Nature Reserve by principal component and path analysis methods. *Environ Sci Pollut Res* 25:2320–2330. <https://doi.org/10.1007/s11356-017-0570-5>
- Horion S, Ivits E, Keersmaecker De et al (2019) Mapping European ecosystem change types in response to land-use change, extreme climate events, and land degradation. *Land Degrad Dev* 30:951–963. <https://doi.org/10.1002/ldr.3282>
- Hu Q, Pan FF, Pan XB et al (2015) Spatial analysis of climate change in Inner Mongolia during 1961–2012. *China Appl Geogr* 60:254–260. <https://doi.org/10.1016/j.apgeog.2014.10.009>
- IUSS Working Group WRB (2014) World reference base for soil resources 2014

- Kallenbach CM, Conant RT, Calderón F et al (2019) A novel soil amendment for enhancing soil moisture retention and soil carbon in drought-prone soils. *Geoderma* 337:256–265. <https://doi.org/10.1016/j.geoderma.2018.09.027>
- Li Z, Bagan H, Yamagata Y (2018) Analysis of spatiotemporal land cover changes in Inner Mongolia using self-organizing map neural network and grid cells method. *Sci Total Environ* 636:1180–1191. <https://doi.org/10.1016/j.scitotenv.2018.04.361>
- Li Z, Ma Z, van der Kuijp TJ et al (2014) A review of soil heavy metal pollution from mines in China: pollution and health risk assessment. *Sci Total Environ* 468–469:843–853. <https://doi.org/10.1016/j.scitotenv.2013.08.090>
- Liang Q, Jing H, Gregoire DC (2000) Determination of trace elements in granites by inductively coupled plasma mass spectrometry. *Talanta* 51:507–513. [https://doi.org/10.1016/S0039-9140\(99\)00318-5](https://doi.org/10.1016/S0039-9140(99)00318-5)
- Lindsay WL (1984) Soil and plant relationships associated with iron deficiency with emphasis on nutrient interactions. *J Plant Nutr* 7:489–500. <https://doi.org/10.1080/01904168409363215>
- Lindsay WL, Schwab AP (1982) The chemistry of iron in soils and its availability to plants. *J Plant Nutr* 5:821–840. <https://doi.org/10.1080/01904168209363012>
- Liu ZF, Fu BJ, Zheng XX et al (2010) Plant biomass, soil water content and soil N: P ratio regulating soil microbial functional diversity in a temperate steppe: a regional scale study. *Soil Biol Biochem* 42:445–450. <https://doi.org/10.1016/j.soilbio.2009.11.027>
- Lorenzo P, RodriEcheverría S, González L et al (2010) Effect of invasive *Acacia dealbata* Link on soil microorganisms as determined by PCR-DGGE. *Appl Soil Ecol* 44:245–251. <https://doi.org/10.1016/j.apsoil.2010.01.001>
- Manlay RJ, Chotte JL, Masse D et al (2002) Carbon, nitrogen and phosphorus allocation in agro-ecosystems of a West African savanna: III. Plant and soil components under continuous cultivation. *Agric Ecosyst Environ* 88:249–269. [https://doi.org/10.1016/S0167-8809\(01\)00219-5](https://doi.org/10.1016/S0167-8809(01)00219-5)
- Meyfroidt P, Lambin EF (2011) Global land use change, economic globalization, and the looming land scarcity. *Proc Natl Acad Sci USA* 108:3465–3472. <https://doi.org/10.1073/pnas.1100480108>
- Millaleo R, Reyes-Díaz M, Ivanov AG et al (2010) Manganese as essential and toxic element for plants: transport, accumulation and resistance mechanisms. *J Soil Sci Plant Nutr* 10:470–481. <https://doi.org/10.4067/S0718-95162010000200008>
- Na R, Du H, Na L et al (2019) Spatiotemporal changes in the aeolian desertification of Hulunbuir grassland and its driving factors in China during 1980–2015. *CATENA* 182:104123. <https://doi.org/10.1016/j.catena.2019.104123>
- Nguyen H, Dargusch P, Moss P et al (2016) A review of the drivers of 200 years of wetland degradation in the Mekong Delta of Vietnam. *Reg Environ Change* 16:2303–2315. <https://doi.org/10.1007/s10113-016-0941-3>
- Niu Z-G, Zhang HY, Wang XM et al (2012) Mapping wetland changes in China between 1978 and 2008. *Chin Sci Bull* 57:2813–2823. <https://doi.org/10.1007/s11434-012-5093-3>
- R Core Team (2020) R: a language and environment for statistical computing. R Foundation for Statistical Computing, Vienna, Austria
- Rahman Z, Singh VP (2019) The relative impact of toxic heavy metals (THMs) (arsenic (As), cadmium (Cd), chromium (Cr)(VI), mercury (Hg), and lead (Pb)) on the total environment: an overview. *Environ Monit Assess* 191:419. <https://doi.org/10.1007/s10661-019-7528-7>
- Rillig MC, Mummey DL (2010) Mycorrhizas and soil structure. *New Phytol* 171:41–53. <https://doi.org/10.1111/j.1469-8137.2006.01750.x>
- Risacher F, Alonso H, Salazar C (2003) The origin of brines and salts in Chilean salars: a hydrochemical review. *Earth Sci Rev* 63:249–293. [https://doi.org/10.1016/S0012-8252\(03\)00037-0](https://doi.org/10.1016/S0012-8252(03)00037-0)
- Sarwar N, Imran M, Shaheen MR et al (2017) Phytoremediation strategies for soils contaminated with heavy metals: modifications and future perspectives. *Chemosphere* 171:710–721. <https://doi.org/10.1016/j.chemosphere.2016.12.116>
- Schmidt SB, Jensen PE, Husted S (2016) Manganese deficiency in plants: the impact on photosystem II. *Trends Plant Sci* 21:622–632. <https://doi.org/10.1016/j.tplants.2016.03.001>
- Scudiero E, Skaggs TH, Corwin DL (2016) Comparative regional-scale soil salinity assessment with near-ground apparent electrical conductivity and remote sensing canopy reflectance. *Ecol Indic* 70:276–284
- Seth CS (2012) A review on mechanisms of plant tolerance and role of transgenic plants in environmental clean-up. *Bot Rev* 78:32–62. <https://doi.org/10.1007/s12229-011-9092-x>
- Seth CS, Chaturvedi PK, Misra V (2007) Toxic effect of arsenate and cadmium alone and in combination on giant duckweed (*Spirodela polyrrhiza* L.) in response to its accumulation. *Environ Toxicol* 22:539–549. <https://doi.org/10.1002/tox.20292>
- Shen C, Xiong J, Zhang H et al (2013) Soil pH drives the spatial distribution of bacterial communities along elevation on Changbai Mountain. *Soil Biol Biochem* 57:204–211. <https://doi.org/10.1016/j.soilbio.2012.07.013>
- Soil environmental quality risk control standard for soil contamination of agricultural land. GB 15618–2018, 2018. [http://www.mee.gov.cn/ywgz/fgbz/bz/bzwb/trhj/201807/t20180703\\_446029.shtml](http://www.mee.gov.cn/ywgz/fgbz/bz/bzwb/trhj/201807/t20180703_446029.shtml)
- Soil and sediment-determination of aqua regia extracts of 12 metal elements-inductively coupled plasma mass spectrometry. HJ 803-2016, 2016. [https://www.mee.gov.cn/ywgz/fgbz/bz/bzwb/jeffbz/201606/t20160630\\_356525.shtml](https://www.mee.gov.cn/ywgz/fgbz/bz/bzwb/jeffbz/201606/t20160630_356525.shtml)
- Sun B, Liu Y, Lei Y (2016) Growing season relative humidity variations and possible impacts on Hulunbuir grassland. *Sci Bull* 61:728–736. <https://doi.org/10.1007/s11434-016-1042-x>
- Sun S, Sang W, Axmacher JC (2020) China's national nature reserve network shows great imbalances in conserving the country's mega-diverse vegetation. *Sci Total Environ* 717:137–159. <https://doi.org/10.1016/j.scitotenv.2020.137159>
- Tian S, Liang T, Li K et al (2018a) Source and path identification of metals pollution in a mining area by PMF and rare earth element patterns in road dust. *Sci Total Environ* 633:958–966. <https://doi.org/10.1016/j.scitotenv.2018.03.227>
- Tian SH, Liang T, Li KX, Wang LQ (2018b) Source and path identification of metals pollution in a mining area by PMF and rare earth element patterns in road dust. *Sci Total Environ* 633:958–966. <https://doi.org/10.1016/j.scitotenv.2018.03.227>
- Viehweger K (2014) How plants cope with heavy metals. *Bot Stud* 55:35. <https://doi.org/10.1186/1999-3110-55-35>
- Wichelns D, Qadir M (2015) Achieving sustainable irrigation requires effective management of salts, soil salinity, and shallow groundwater. *Agric Manage Water Qual* 157:31–38
- Xiong J, Liu Y, Lin X et al (2012) Geographic distance and pH drive bacterial distribution in alkaline lake sediments across Tibetan Plateau. *Environ Microbiol* 14:2457–2466. <https://doi.org/10.1111/j.1462-2920.2012.02799.x>
- Xu W, Xiao Y, Zhang J et al (2017) Strengthening protected areas for biodiversity and ecosystem services in China. *Proc Natl Acad Sci USA* 114:1601–1606. <https://doi.org/10.1073/pnas.1620503114>
- Yang Y, Wang ZQ, Li JL et al (2016) Comparative assessment of grassland degradation dynamics in response to climate variation and human activities in China, Mongolia, Pakistan and Uzbekistan from 2000 to 2013. *J Arid Environ* 135:164–172. <https://doi.org/10.1016/j.jaridenv.2016.09.004>
- Yaylali-Abanuz G (2011) Heavy metal contamination of surface soil around Gebze industrial area. *Turkey Microchem J* 99:82–92. <https://doi.org/10.1016/j.microc.2011.04.004>
- Yinglan A, Wang G, Liu T et al (2019) Vertical variations of soil water and its controlling factors based on the structural equation

- model in a semi-arid grassland. *Sci Total Environ* 691:1016–1026. <https://doi.org/10.1016/j.scitotenv.2019.07.181>
- Yu X, Chang Z, Jie X (2015) Areas benefiting from water conservation in key ecological function areas in China. *J Resour Ecol* 6:375–385. <https://doi.org/10.5814/j.issn.1674-764x.2015.06.005>
- Zhang F, Yu A, Jing Y (2019a) Assessing and predicting changes of the ecosystem service values based on land use/cover change in Ebinur Lake Wetland National Nature Reserve, Xinjiang. *China Sci Total Environ* 656:1133–1144. <https://doi.org/10.1016/j.scitotenv.2018.11.444>
- Zhang H, Wang ZF, Zhang YL, Hu ZJ (2012) The effects of the Qinghai-Tibet railway on heavy metals enrichment in soils. *Sci Total Environ* 439:240–248. <https://doi.org/10.1016/j.scitotenv.2012.09.027>
- Zhang P, Qin C, Hong X et al (2018) Risk assessment and source analysis of soil heavy metal pollution from lower reaches of Yellow River irrigation in China. *Sci Total Environ* 633:1136–1147. <https://doi.org/10.1016/j.scitotenv.2018.03.228>
- Zhang Q, Tang HP, Cui FQ et al (2019) SPEI-based analysis of drought characteristics and trends in Hulun Buir grassland. *Acta Ecol. Sin* 39: 7110–7123. <https://doi.org/10.5846/stxb201807061481>
- Zhou Y, Dong JW, Xiao XM et al (2019) Continuous monitoring of lake dynamics on the Mongolian Plateau using all available Landsat imagery and Google Earth Engine. *Sci Total Environ* 689:366–380. <https://doi.org/10.1016/j.scitotenv.2019.06.341>
- Zhu Y, Zhang Z, Zhao X et al (2017a) Accumulation and potential sources of heavy metals in the soils of the Hetao irrigation district, Inner Mongolia, China. *Pedosphere* 30:245–252. [https://doi.org/10.1016/s1002-0160\(17\)60306-0](https://doi.org/10.1016/s1002-0160(17)60306-0)
- Zhu YC, Zhang ZH, Zhao XY, Lian J (2017b) Accumulation and potential sources of heavy metals in the soils of the Hetao irrigation district, Inner Mongolia, China. *Pedosphere* S1002016017603060. [https://doi.org/10.1016/s1002-0160\(17\)60306-0](https://doi.org/10.1016/s1002-0160(17)60306-0)

**Publisher's Note** Springer Nature remains neutral with regard to jurisdictional claims in published maps and institutional affiliations.

## Authors and Affiliations

Junyong Ma<sup>1,2,3</sup> · Zhenzhen Hao<sup>1,2</sup> · Yibo Sun<sup>1,2</sup> · Bo Liu<sup>1,2</sup> · Wenjie Jing<sup>1,2</sup> · Jiaqiang Du<sup>1,2</sup> · Junsheng Li<sup>1,2</sup>

Junyong Ma  
mjj172404707@me.com

Zhenzhen Hao  
haozhzh96@163.com

Yibo Sun  
sunyb68@163.com

Bo Liu  
liubo@craes.org.cn

Wenjie Jing  
15232033@163.com

Jiaqiang Du  
31927023@qq.com

<sup>1</sup> State Key Laboratory of Environmental Criteria and Risk Assessment, Chinese Research Academy of Environmental Sciences, Beijing 100012, China

<sup>2</sup> State Key Laboratory of Environmental Protection for Regional Eco-Process and Function Assessment, Chinese Research Academy of Environmental Sciences, Beijing 100012, China

<sup>3</sup> China Institute for Geo-Environmental Monitoring, Beijing 100081, China